A Numerical Study on Natural Ventilation Using a Horizontal Solar Chimney with a Bell-Mouth Inlet and Major Geometric Modifications

Do Ngoc Kien
Faculty of Heat and Refrigeration Engineering, Industrial University of Ho Chi Minh City (IUH), Vietnam
ngockien.mvac@gmail.com

Minh Phu Nguyen
Faculty of Heat and Refrigeration Engineering, Industrial University of Ho Chi Minh City (IUH), Vietnam
nguyenminhphu@iuh.edu.vn

Thi Tam Thanh Nguyen
Faculty of Heat and Refrigeration Engineering, Industrial |University of Ho Chi Minh City (IUH), Vietnam
nguyenthitamthanh@iuh.edu.vn (corresponding author)

Received: 17 September 2025 | Revised: 27 October 2025 | Accepted: 3 November 2025

 DOI: https://doi.org/10.48084/etasr.14861

ABSTRACT

A numerical study was conducted to examine the natural ventilation performance of a horizontal solar chimney connected to a confined space. The study analyzed the impact of geometric modifications on the air mass flow rate. Four designs were examined using the Computational Fluid Dynamics (CFD) model: a Base Case (BC), a Radius Elbow (RE), a Bell Mouth (BM), and a combined Bell Mouth and Radius Elbow (BMRE). The BM inlet and the RE, significantly improved aerodynamic efficiency by reducing flow separation and pressure losses. The BMRE design reached the highest air mass flow rate of approximately 0.0425 kg/s at a heat flux of 800 W/m², which is a significant increase compared to the BC's flow rate of 0.039 kg/s. These results confirm that optimizing the geometries of the inlet and elbow can improve the efficiency of passive solar ventilation systems.

Keywords-solar chimney; natural ventilation; Computational Fluid Dynamics (CFD); bell-mouth inlet; mass flow rate

I. INTRODUCTION

Natural ventilation can be used for maintaining thermal comfort in buildings, but it is influenced by factors, such as openings, building orientation, and appropriate materials, in order to allow optimal airflow and temperature stability, especially in tropical climates [1-3]. A solar chimney is a system designed to improve natural ventilation and provide heating, based on the stack effect, also known as thermal buoyancy. A typical solar chimney is a vertical shaft with a transparent cover and a dark, heat-absorbing wall [4]. As the sun heats the dark surface, the air inside the chimney becomes warmer and less dense than the air in the building, rising through an opening at the top. A negative pressure is created at the base, drawing in cooler, fresh air through lower-level openings, such as windows or vents, creating a continuous airflow [5]. In colder climates, the same principle can be used for heating. Closing the top vent of the chimney and opening a vent into the building's interior circulates the heated air from the chimney back into the building, providing passive solar heating. Some designs also include heat storage materials that release warmth at night [6, 7].

The greatest advantage of a horizontal solar chimney is its ability to integrate it into the roof, using the entire surface area for thermal absorption, even when the sunlight is indirect. Furthermore, it provides shading and protection for the roof, while improving the efficiency of air conditioning systems. A horizontal chimney can be combined with other systems, such

as photovoltaic panels, to optimize both ventilation and electricity generation [8-10]. The BM inlet plays a crucial role in improving performance by guiding the airflow smoothly and efficiently into the duct [11]. The curved shape reduces flow separation and pressure losses at the intake, allowing the chimney to operate more efficiently [12]. By optimizing the air intake, the BM inlet increases the overall volume of air passing through the device. This creates a more uniform velocity profile at the inlet, preventing the formation of vortices and turbulence, which can reduce performance and increase noise [13, 14]. Integrating a BM design into the inlet of a natural convection Solar Air Heater (SAH) increases the air mass flow rate by creating a ram-air effect [15]. This design converts dynamic pressure into static pressure, significantly increasing the air flow rate and improving heat transfer with minimal hydraulic losses.

Authors in [15] found that certain BM designs can increase the flow rate by over 100% compared to conventional flat plate solar air heaters, making them more suitable for applications requiring a high flow of heated air. Authors in [16] focused on improving the thermal performance of these systems, often at the expense of aerodynamic efficiency due to high pressure losses by proposing and examining a design modification: the integration of a BM inlet to improve the aerodynamic efficiency of a coupled Trombe wall-SAH system for rapid space heating. Authors in [17] presented a novel design with a BM inlet to improve the aerodynamic efficiency of natural convection SAHs. While some research has explored different inlet designs for solar chimneys by changing the direction of the inlet plane, no detailed analysis has been conducted on a smooth flat plate SAH with a BM integrated design. A BM has also been integrated into solar power plants [18, 19]. Authors in [20] showed that strategically placing a deflector at the base of a solar chimney's collector enhanced ventilation performance and thermal efficiency by 8.2% and 7.4%, respectively. Authors in [21] noted that the predicted natural ventilation rate and heat transfer coefficient depended on the size of the computational domain. In a 3-m-tall, 0.6-m-wide cavity with symmetrical heating, the flow rate predicted using the large domain was nearly 40% larger than the rate predicted using the small one. For a symmetrically heated cavity, the authors proposed an extension of about 3 m (five times the cavity width), and for an asymmetrically heated cavity, an extension of about 6 m (ten times the width) to limit the error within 0.5%. Authors in [22] analyzed a novel hybrid system that included a sloped solar chimney within the building's roof. This inclined chimney heats air from the room and helps drive an adsorption chiller and a desalination unit. Authors in [23] investigated a vertical solar chimney, referring to it as a wall solar chimney or solar façade. Their analysis focused on this vertical, wall-integrated design, considering the effects of solar irradiance, air gap dimension, and ambient temperature. However, the literature lacks a comprehensive numerical study that combines both horizontal solar chimneys for ventilation and BM inlets in solar air heaters to enhance flow.

Existing studies often focus on either thermal or aerodynamic efficiency. Thus, a detailed analysis is needed to understand how a BM inlet in a horizontal solar chimney impacts both simultaneously, along with key performance indicators such as mass flow rate. Specifically, systematic parametric analysis is required to optimize the key geometric parameters of the BM inlet and the horizontal solar chimney duct (e.g., mitered elbow, radius elbow) to maximize ventilation performance. This paper presents a horizontal solar chimney, which differs from coupled Trombe wall-SAH systems. It focuses on roof integration and uses a horizontal flow path primarily for natural ventilation. It also explores optimizations, such as BM inlets and radius elbows, to improve airflow through the necessary bends. In contrast, other studies analyze systems that combine an inclined SAH with a vertical Trombe wall or enhance a standard inclined SAH with a vertical chimney. These systems aim to maximize the flow of the heated air for rapid space heating or to improve the overall thermohydraulic performance through specific inlet designs, like bell mouths at the SAH and Trombe channel entries, or channel modifications, like tapering. While they all leverage passive solar principles, they differ significantly in orientation, component integration, and primary performance goals.

II. MODEL DESCRIPTION

Figure 1 shows the 2D numerical models that were used to study natural ventilation with a horizontal solar chimney. The standalone model is a simplified approach to studying a solar chimney, focusing on the channel of the chimney under the assumption that the inlet and outlet are directly exposed to the ambient environment.

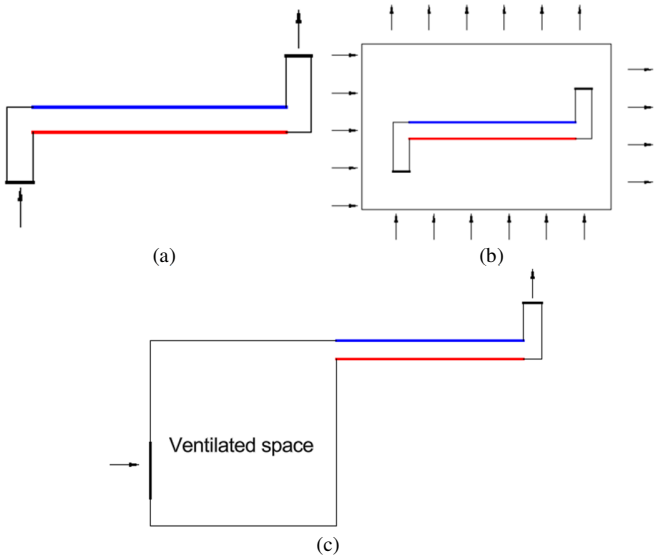

Fig. 1. Types of computational domain to study a solar chimney: (a) standalone model, (b) large extended model, (c) attached model.

This method was common in early studies because it simplified the computational domain. In contrast, the large extended model is much larger than the physical cavity and has extensions on all sides. This extended domain allows the chimney to be simulated as if it was immersed in air, providing a more realistic representation of the flow. Additionally, using this domain can account for phenomena, such as the distortion of incoming air or significant reverse flow at the outlet, which can occur in wider, asymmetrically heated cavities. The

attached model is considered more realistic because it integrates the solar chimney with a ventilated space, or a room. Therefore, this model accounts for the interaction between the chimney and the room, including the pressure drop and flow dynamics that occur as air is drawn from the room and exhausted through the chimney. Authors in [24] concluded that using an attached model is crucial for obtaining more realistic and accurate predictions of a solar chimney's ventilation performance because it better simulates real-world conditions. Therefore, the attached model is used in the current study.

Figure 2 shows the four computational cases used to study a horizontal solar chimney connected to a ventilated space.

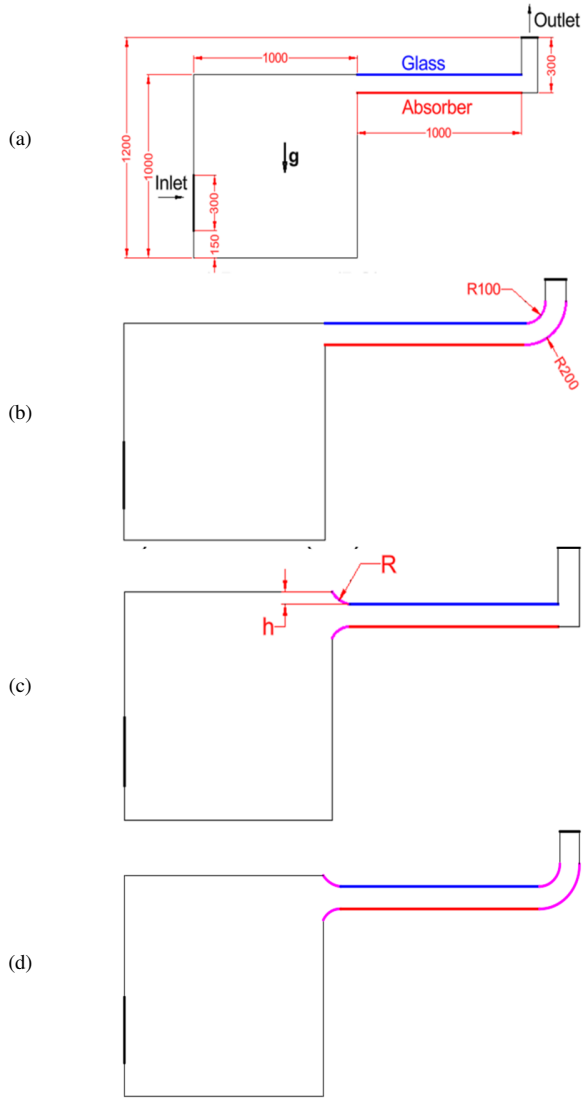

Fig. 2. Computational domain for the ventilated space using a horizontal solar chimney (the attached model) of various cases: (a) BC, (b) RE, (c) BM, (d) BMRE.

The vector g represents the direction of gravitational acceleration. The BC features a sharp-edged inlet and a mitered elbow that connects the horizontal solar chimney, which includes a glass cover and an absorber plate. The RE case modifies the BC by replacing the sharp mitered elbow with a smooth, curved elbow. The BM case includes a BM inlet at the channel's entry while retaining the mitered elbow from the BC. Finally, the BMRE combines the two design improvements and for the parametric study, the ranges of the bell mouth's protruding height (h) and arc radius (R) are 10 mm-100 mm and 50 mm-100 mm, respectively. The horizontal solar chimney channel is 1000 mm long and 100 mm high. The channel height is the vertical distance between the upper glass surface and the lower absorber plate. The horizontal channel connects to a 300-mm-high vertical riser section that leads to the outlet. The chimney is attached to a 1000 mm × 1000 mm space featuring a 300 mm tall air inlet positioned 150 mm from the bottom.

Figure 3 displays the mesh used for the numerical simulation, which is a grid of small elements that is used to divide the computational domain into smaller parts for the ANSYS. It is structured and composed of quadrilateral elements throughout the ventilated space, horizontal channel, and vertical riser. The total number of elements is approximately 114,480, the overall view shows the entire model, and the magnified view highlights the mesh refinement at the glass or absorber surfaces. This refinement, where the mesh elements are smaller and more numerous, is crucial for accurately capturing the steep temperature and velocity gradients that occur near these surfaces. A grid independence test was performed to ensure that the numerical results are not dependent on the mesh size. The study evaluated the sensitivity of the predicted mass flow rate and average air temperature rise through the chimney to different mesh densities, represented by maximum $y+$ values. The results showed that the flow rate and temperature rise became independent of the mesh size when the maximum $y+$ value was less than 2.0, ensuring grid-independent results in the following simulations.

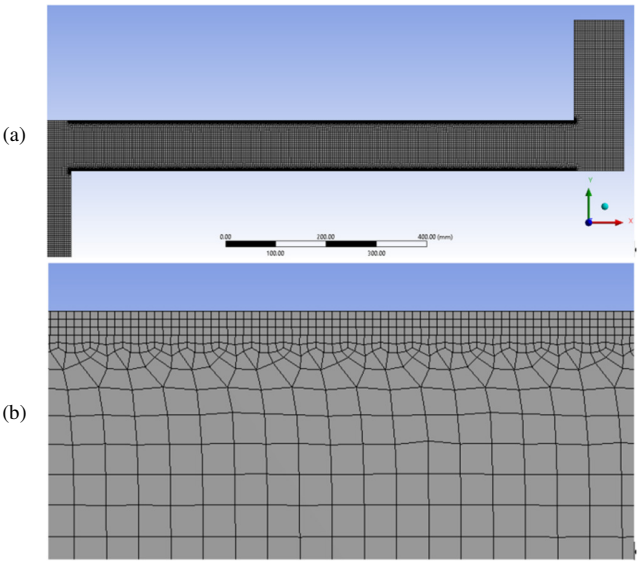

Fig. 3. (a) Mesh generation with refinement at glass and (b) absorber surfaces.

This study used the numerical methodology with the ANSYS Fluent solver to simulate natural ventilation. The SST *k-ω* turbulence model was selected to measure the flow, and the S2S radiation model was used to simulate heat transfer between surfaces. The flow inside the solar chimney channel is mostly laminar. However, when the thermal flow exits the channel, it behaves as a free buoyant jet where turbulence may occur. The SST *k-ω* model was adopted specifically to simulate these mixed laminar and turbulent flows, both inside and outside the air channel. The SST *k-ω* model uses a blending function, combining the advantages of two models by activating the *k-ω* model in the near-wall region, where it performs well, and applying the *k-ε* model to the rest of the domain. Authors in [25] showed that the SST *k-ω* model agreed well with the experimental measurements. Air was treated as an ideal gas with fixed properties: specific heat (1006.43 J/kg-K), thermal conductivity (0.0242 W/m-K), and viscosity (1.7894×10^{-5} kg/m-s). The simulation was considered converged when all residuals reached 10^{-3}, except for the energy equation, for which a stricter convergence criterion of 10^{-6} was used. The SST k-ω turbulence model and the S2S radiation model are [26]:

- Transport equation for turbulent kinetic energy (k):

$$\frac{\partial(\rho k)}{\partial t}+\frac{\partial(\rho k u_i)}{\partial x_i}=\frac{\partial}{\partial x_j}\left[\left(\mu+\frac{\mu_t}{\sigma_k}\right)\frac{\partial k}{\partial x_j}\right]+G_k-Y_k+S_k \quad (1)$$

- Transport equation for specific dissipation rate (ω):

$$\frac{\partial(\rho\omega)}{\partial t}+\frac{\partial(\rho\omega u_i)}{\partial x_i}=\frac{\partial}{\partial x_j}\left[\left(\mu+\frac{\mu_t}{\sigma_{\omega,i}}\right)\frac{\partial\omega}{\partial x_j}\right]+G_\omega-Y_\omega+D_\omega+S_\omega \quad (2)$$

$$J_i=\varepsilon_i\sigma T_i^4+(1-\varepsilon_i)\sum_{j=1}^{N}F_{ij}J_j \quad (3)$$

where (J) is the radiosity of each surface, the total radiative energy leaving a surface.

$$F_{ij}=\frac{1}{A_i}\int_{A_i}\int_{A_j}\frac{cos\theta_i cos\theta_j}{\pi r^2}dA_j dA_i \quad (4)$$

where F_{ij} is the view factor, a purely geometric quantity for the S2S model.

A boundary condition is a set of physical constraints or values that are applied to the edges of a computational area in order to solve partial differential equations. For the numerical study, the inlet boundary condition is defined as a pressure inlet, while the outlet boundary condition is defined as a pressure outlet. The glass surface is adiabatic with an emissivity of 0.86, and the absorber surface is set as a heat flux boundary ranging from 300 W/m² to 800 W/m² for the parametric study with an emissivity of 0.95 [25]. No-slip boundary conditions were applied to the other walls, which were assumed to be adiabatic. Figures 4 and 5 validate the numerical model by comparing the results with previous studies. Figure 4 displays the temperature distribution at a heat flux of 800 W/m² for the attached model used in this study and the large extended model from [8]. The results demonstrate a similar temperature profile trend. Figure 5 shows a maximum deviation of 8.2%, confirming that the attached model used in the current study reliably predicts the performance of a solar chimney. However, the mass flow rate in this study is up to 8.2% higher than in the previous work. This discrepancy can be attributed to the different computational models used. The present research uses an attached model that integrates the solar chimney with a ventilated space or a room. This provides a more realistic representation of real-world conditions. This setup accounts for the pressure drop and flow dynamics as air is drawn from a confined space, effectively creating a more significant pressure difference that drives the stack effect.

III. RESULTS AND DISCUSSION

The study examines a range of key parameters, including heat flux from 300 W/m² to 800 W/m², BM arc radii of 50 mm and 100 mm, and protruding heights of the BM from 10 mm to 100 mm.

A. *Effects of Designs and Heat Flux*

Figure 6 illustrates the velocity distribution of four horizontal solar chimney designs with a heat flux of 800 W/m². The BC, with its sharp-edged inlet and mitered elbow, produces a less uniform velocity profile, especially near the elbow, where the sharp turn causes flow separation and turbulence.

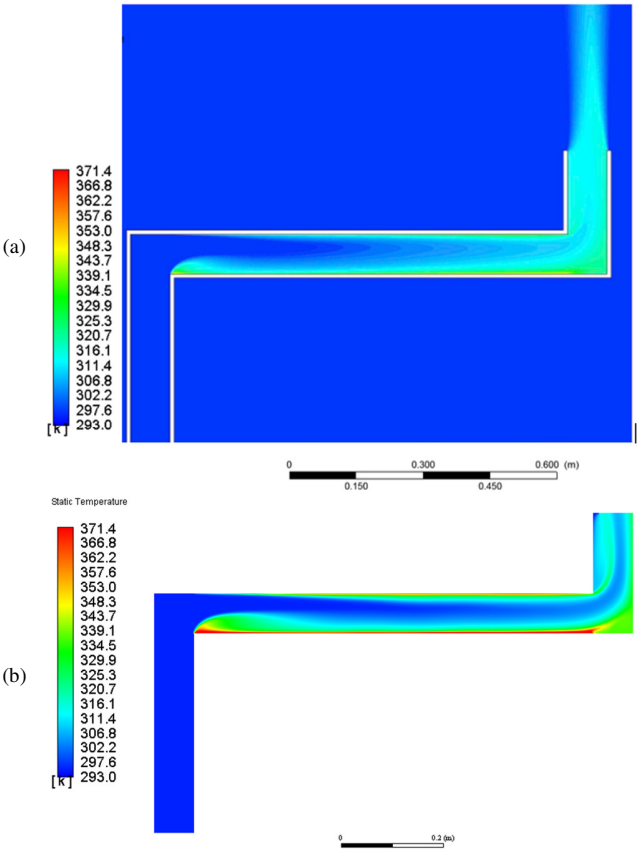

Fig. 4. Comparison of temperature distribution at heat flux of 800 W/m^2: (a) large extended model [8], (b) attached model.

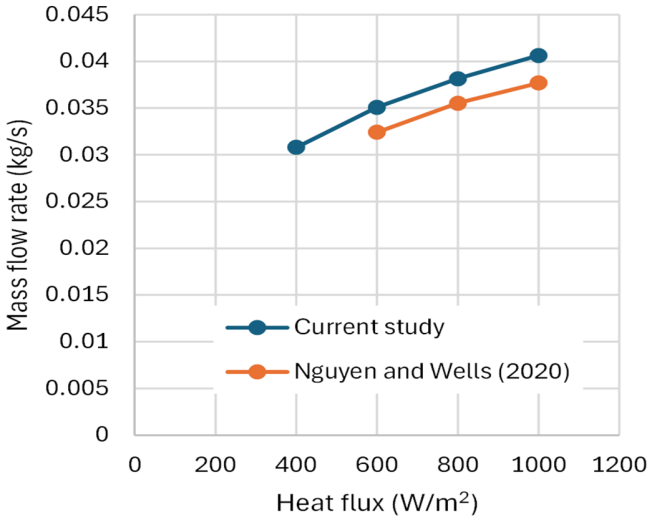

Fig. 5. Comparison of induced mass flow rate.

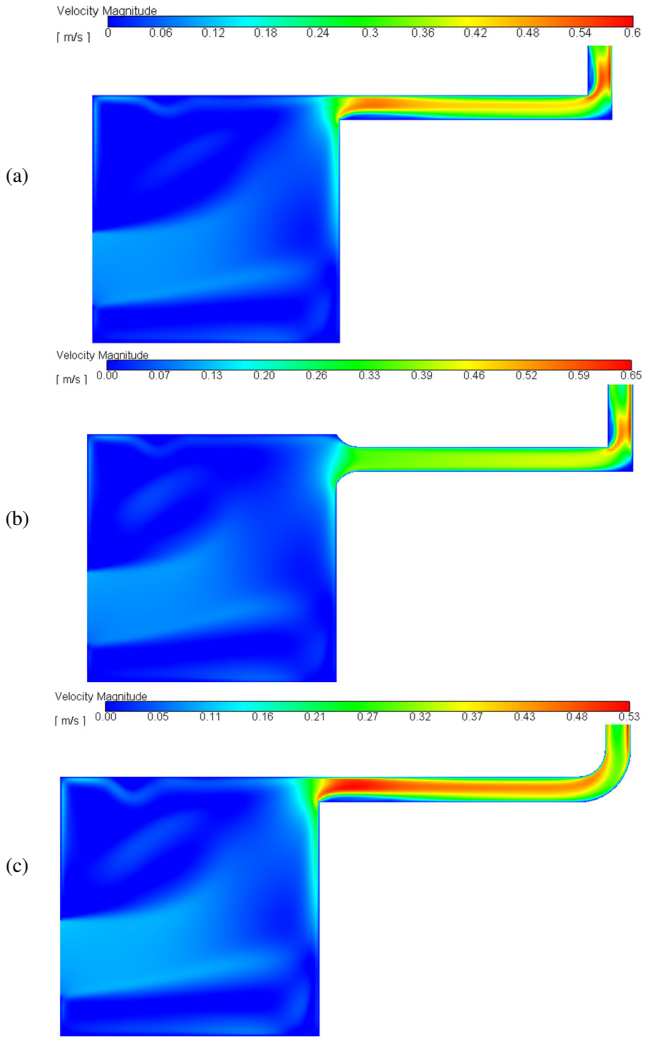

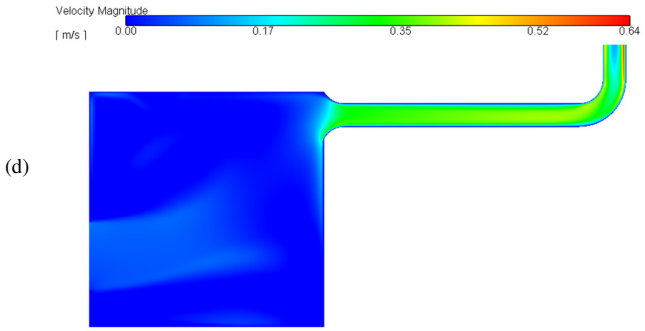

Fig. 6. Velocity distribution for various designs of horizontal solar chimney (800 W/m^2, R = 100 mm, h = 50 mm): (a) BC, (b) BM inlet, (c) RB, (d) BMRE.

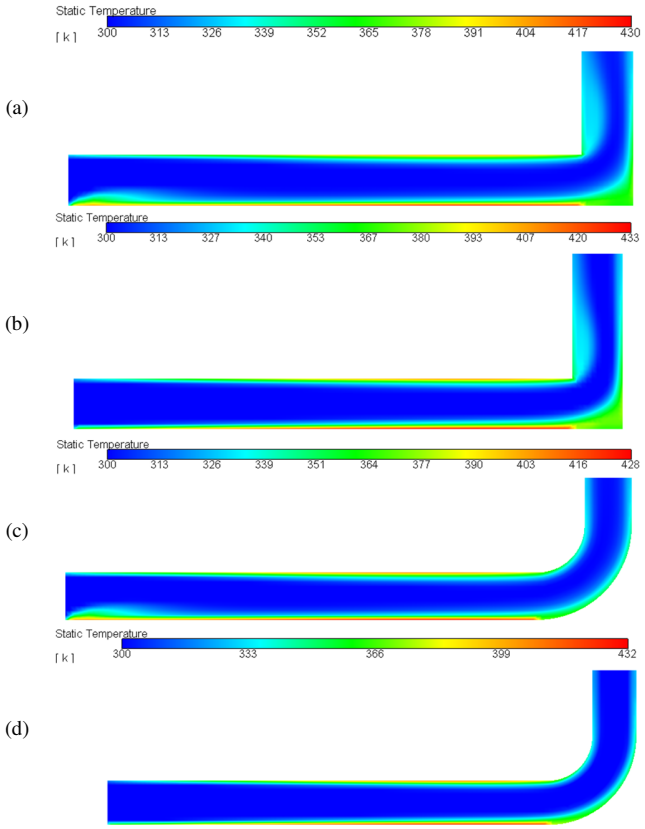

Fig. 7. Temperature distribution for various designs of horizontal solar chimney (800 W/m^2, R = 100 mm, h = 50 mm): (a) BC, (b) BM inlet, (c) RB, (d) BMRE.

In contrast, the RE case uses a smooth, curved elbow and has a much smoother, more uniform velocity distribution. This reduces pressure losses and improves flow efficiency as the air flows through the turn. Similarly, the BM inlet case, which has a bell-shaped inlet and a mitered elbow, exhibits a more uniform velocity profile at the intake, increasing the overall volume of air passing through the device. The smooth, curved shape of the BM inlet reduces flow separation and pressure losses at the intake, enabling the chimney to operate more efficiently. The most effective design is the BMRE case, which combines these improvements. The velocity distribution in this design is the most uniform and streamlined throughout the

entire channel, from the inlet to the outlet. The BM inlet guides airflow smoothly into the channel, and the RE reduces pressure drops and turbulence associated with changes in direction. This combination results in a higher, more efficient mass flow rate compared to other designs. Figure 7 portrays the temperature distribution for the four solar chimney designs with a heat flux of 800 W/m².

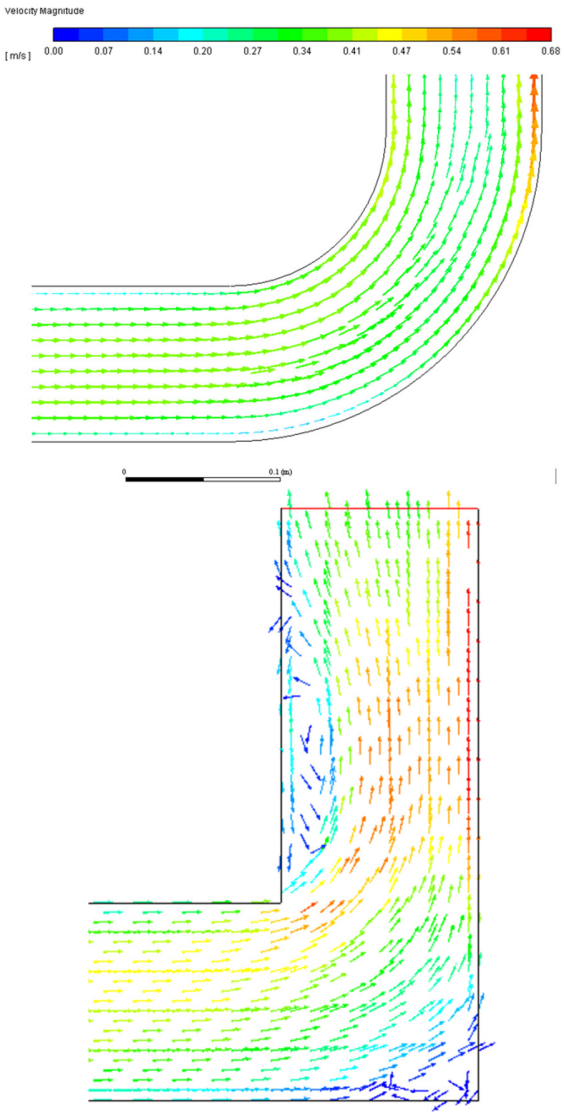

Fig. 8. Velocity vector of elbows: (a) radius, (b) mitered.

The BC and RE models lack a BM inlet. Consequently, the air entering these models creates a turbulent flow, or vortex, at the sharp corner. This vortex traps air, leading to a localized rise in temperature at the inlet area. In contrast, the BM and BMRE models have much smoother and more uniform flow at the inlet with no noticeable vortex or temperature buildup. The BM inlet significantly reduces flow separation and pressure losses. This allows air to enter the channel more efficiently, preventing the formation of stagnant, high-temperature zones. The air trapped within this vortex has a lower velocity and remains in contact with the warm surfaces longer, causing its temperature to rise relative to the main, cooler airflow. Conversely, the curved BM inlet in the BM and BMRE designs is aerodynamically optimized to guide air smoothly and efficiently into the channel. This prevents flow separation and vortex formation, resulting in a more uniform velocity profile and a cooler, more stable temperature at the inlet. Figure 8 provides a comparison of the velocity vectors for two types of elbows used in solar chimney designs: the RE and the mitered elbow.

The flow is smooth for the RE and follows the curve of the elbow, with the vectors remaining parallel to the walls. In contrast, the mitered elbow causes the airflow to separate from the inner wall due to its sharp, 90-degree turn, creating a large, chaotic vortex. These contrasting flow patterns have significant implications for the solar chimney's performance. The smooth, well-guided flow of the RE is characteristic of a low-pressure-loss component. By preventing flow separation and minimizing turbulence, the RE preserves the kinetic energy of the air efficiently as it changes direction. This smooth transition reduces the overall pressure drop across the elbow, enabling a higher air mass flow rate driven by the stack effect. Conversely, the vortex formed in the mitered elbow is a major source of hydraulic loss. The sharp turn forces the air to separate from the inner wall, creating a region of recirculating flow. This turbulent, chaotic motion dissipates energy and significantly increases the pressure drop across the elbow. The result is a much less efficient system because more of the buoyancy-induced pressure difference is consumed overcoming flow resistance than driving ventilation through the chimney. Figure 9 depicts a visual comparison of the velocity vectors for a BM inlet and a BC inlet. The BM inlet exhibits smooth, uniform airflow with vectors that enter the chimney in a streamlined fashion. This indicates that the curved design effectively guides the air and minimizes flow separation and turbulence. In contrast, the sharp edge of the BC inlet causes the airflow to separate, creating a large, unstable vortex at the corner. This vortex reduces the effective inlet area, increases pressure losses, and can lead to increased noise. The BM's ability to create a more uniform velocity profile and reduce pressure losses enables a significantly higher air volume to pass through the device.

Figure 10 presents the air mass flow rate for four solar chimney designs with varying heat fluxes ranging from 300 W/m² to 800 W/m². The mass flow rate increases with heat flux for all designs. This is due to the stack effect: a higher heat flux increases the temperature difference between the air inside and outside the chimney, strengthening the thermal buoyancy and, consequently, the airflow. The BMRE design yields the highest mass flow rate consistently, reaching approximately 0.0425 kg/s at 800 W/m². This result highlights the benefits of combining a smooth BM inlet with an RE to reduce pressure losses and improve aerodynamic efficiency. The BM design performs second best, followed by the RE, then the BC, which has the lowest flow rate due to combined pressure losses from its sharp inlet and mitered elbow. The significant difference in mass flow rate between the most and least efficient designs demonstrates the importance of geometric modifications for optimizing ventilation performance.

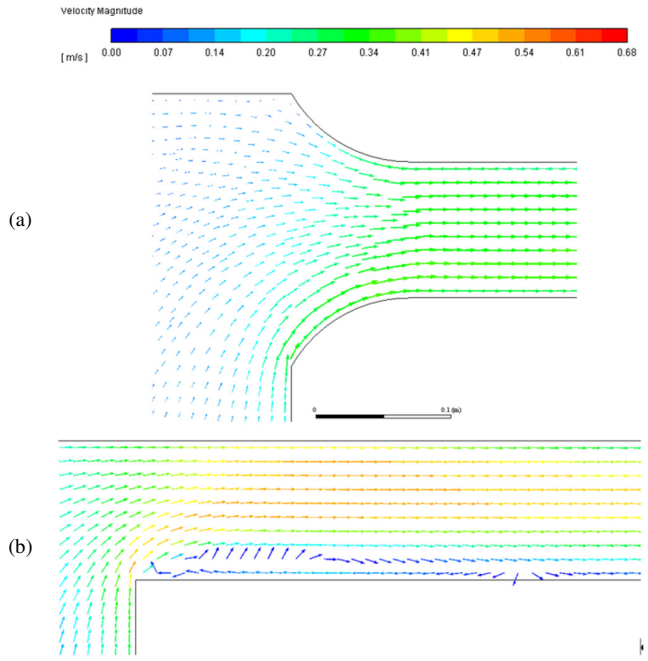

Fig. 9. Velocity vector of chimney inlets: (a) BM, (b) BC.

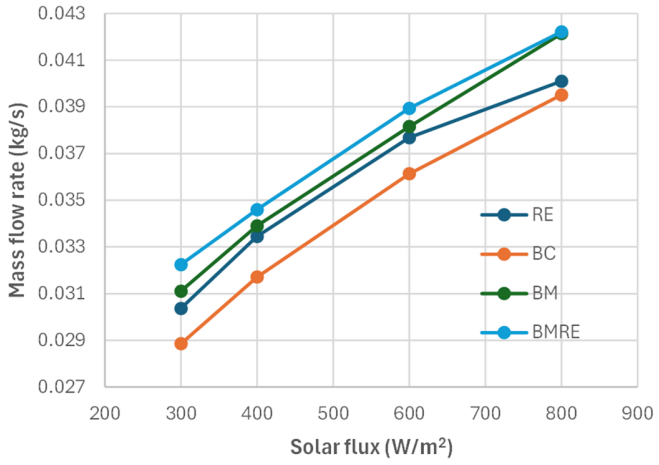

Fig. 10. Air mass flow rate with various designs and heat fluxes (R = 100 mm, h = 50 mm).

B. Effects of the Shape of the Bell Mouth

Figure 11 shows the air velocity profile at the inlet of the BMRE chimney design, examining the effect of varying the protruding height of the BM (h) at a fixed arc radius (R = 100 mm) and heat flux of 800 W/m². Figure 11 shows the velocity across the inlet (from 0 to 0.1 m) and reveals that larger protruding heights result in a more uniform velocity profile. The maximum air velocity increases with height, rising from approximately 0.40 m/s at h = 25 mm to about 0.43 m/s at h = 100 mm. A larger protruding height enables the BM to direct the incoming air more efficiently and smoothly into the channel. This reduces flow separation at the intake and creates a more uniform velocity profile. This profile is crucial for maximizing the overall air mass flow rate through the chimney. The smoother flow and higher velocity achieved with a larger protruding height directly translate to improved ventilation performance because the system can draw a greater volume of fresh air into the ventilated space. Figure 12 presents the air mass flow rate for the BMRE design and how it is affected by the protruding height (h) and arc radius (r) of the BM at a constant heat flux of 800 W/m².

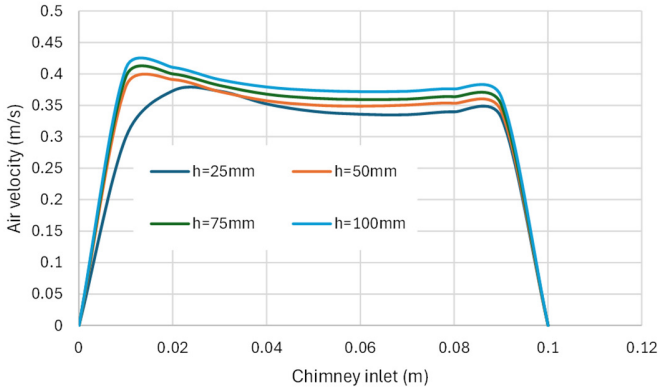

Fig. 11. Velocity profile at the inlet of the BMRE with protruding heights of the BM at a fixed BM arc radius of R = 100 mm and a heat flux of 800 W/m².

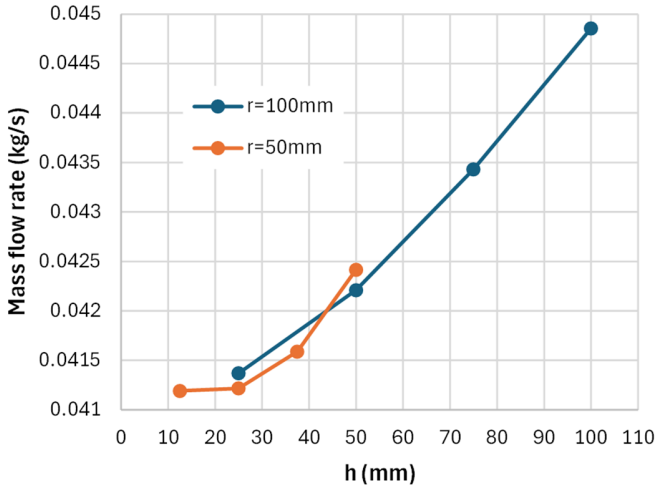

Fig. 12. Air mass flow rate of the BMRE with protruding heights and BM arc radii at 800 W/m² heat flux.

As Figure 12 shows, for both tested radii, the mass flow rate generally increases as the protruding height increases. Specifically, the line for the 100-mm arc radius shows a steady increase in mass flow rate, rising from approximately 0.0415 kg/s at 25 mm to around 0.045 kg/s at 100 mm. The r = 50 mm line follows a similar trend, though its peak performance occurs at a lower height. Increasing the protruding height improves airflow into the chimney by reducing hydraulic losses and creating a more uniform velocity profile, resulting in a higher air mass flow rate. The bell mouth's smooth, curved shape is crucial for converting dynamic pressure into static pressure, significantly boosting the flow rate and improving heat transfer with minimal hydraulic losses. The graph confirms that an optimal design configuration exists: a larger protruding height

allows for more efficient air intake, enhancing the chimney's overall ventilation performance.

IV. CONCLUSIONS

This study examined various horizontal solar chimney designs and concluded that geometric modifications significantly improve ventilation performance by enhancing hydraulic efficiency. Integrating a Bell-Mouth (BM) inlet and a Radius Elbow (RE) proved highly effective because both features reduce pressure losses, minimizing flow separation and turbulence. The design incorporating the Bell Mouth and Radius Elbow (BMRE) consistently achieved the highest air mass flow rates, reaching approximately 0.0425 kg/s at a heat flux of 800 W/m². This rate is significantly higher than that of the traditional horizontal solar chimney (Base Case (BC)), which only reached approximately 0.039 kg/s under the same conditions. Furthermore, optimizing the protruding height and arc radius of the BM further boosted performance, with the mass flow rate peaking at approximately 0.045 kg/s, with a protruding height of 100 mm and an arc radius of 100 mm. This research demonstrates that simple design modifications can highly improve building ventilation, offering a more effective passive cooling solution.

REFERENCES

[1] M. Haiqal, L. H. Sari, H. Husin, A. Akhyar, A. Munir, and K. Bilqis, "The Thermal Comfort Performance in an Indonesian Refugee Tent: Existing Conditions and Redesigns," *Energies*, vol. 18, no. 5, Jan. 2025, Art. no. 1249, https://doi.org/10.3390/en18051249.

[2] M. Muslimsyah, S. Safwan, and A. Akhyar, "Simulations of Temperature and Wind Speed Contours and Vectors for Thermal Comfort Analysis in Worship Spaces: The Case Study of Baiturrahman Grand Mosque, Indonesia," *Engineering, Technology & Applied Science Research*, vol. 15, no. 4, pp. 25199–25206, Aug. 2025, https://doi.org/10.48084/etasr.11734.

[3] M. Muslimsyah, H. Husin, and A. Akhyar, "Numerical analysis of thermal comfort behavior in Acehnese traditional houses in Indonesia," *Ecological Engineering & Environmental Technology*, vol. 26, no. 5, pp. 27–42, May 2025, https://doi.org/10.12912/27197050/202655.

[4] Q. Wang, G. Zhang, Q. Wu, and L. Shi, "Solar chimney under three heating modes," in *Multifunctional Solar Chimney*, 1st ed., L. Shi, Ed. Elsevier, 2025, pp. 71–94.

[5] F. Nasri, "Numerical Simulation of a Efficient Solar-Powered Ventilation System," *Engineering, Technology & Applied Science Research*, vol. 13, no. 4, pp. 11459–11465, Aug. 2023, https://doi.org/10.48084/etasr.6038.

[6] N. M. Phu, N. H. Kha, and N. V. Hap, "Impact of the V CAP on induced turbulent air flow in a solar chimney: a computational study," *Journal of Thermal Engineering*, pp. 520–527, Apr. 2023, https://doi.org/10.18186/thermal.1285240.

[7] C. T. Hau, D. T. H. Hai, N. Van Hap, and N. M. Phu, "One-Dimensional and Entropy Generation Analyses of a Solar Chimney," in *The AUN/SEED-Net Joint Regional Conference in Transportation, Energy, and Mechanical Manufacturing Engineering*, Singapore, 2022, pp. 211–219, https://doi.org/10.1007/978-981-19-1968-8_17.

[8] Y. Q. Nguyen and J. C. Wells, "A numerical study on induced flowrate and thermal efficiency of a solar chimney with horizontal absorber surface for ventilation of buildings," *Journal of Building Engineering*, vol. 28, Mar. 2020, Art. no. 101050, https://doi.org/10.1016/j.jobe.2019.101050.

[9] E. Hadji, B. Ndiogou, S. Tigampo, A. Thiam, and D. Azilinon, "Optimization of a Solar Chimney with a Horizontal Absorber for Building Ventilation: A Case Study," *Fluid Dynamics & Materials Processing*, vol. 19, no. 4, pp. 901–910, 2022, https://doi.org/10.32604/fdmp.2022.021973.

[10] Y. Q. Nguyen and T. N. Huynh, "Evaluating the Performance of a Combined Vertical Wall–Horizontal Roof Solar Chimney for the Natural Ventilation of Buildings," *Buildings*, vol. 14, no. 6, June 2024, Art. no. 1501, https://doi.org/10.3390/buildings14061501.

[11] L.-M. Tam and A. J. Ghajar, "The unusual behavior of local heat transfer coefficient in a circular tube with a bell-mouth inlet," *Experimental Thermal and Fluid Science*, vol. 16, no. 3, pp. 187–194, Mar. 1998, https://doi.org/10.1016/S0894-1777(97)10019-X.

[12] H. Wang, J. Tian, H. Ouyang, Y. Wu, and Z. Du, "Aerodynamic performance improvement of up-flow outdoor unit of air conditioner by redesigning the bell-mouth profile," *International Journal of Refrigeration*, vol. 46, pp. 173–184, Oct. 2014, https://doi.org/10.1016/j.ijrefrig.2014.08.015.

[13] S. Kim, S. Heo, C. Cheong, and T.-H. Kim, "Numerical and experimental investigation of the bell-mouth inlet design of a centrifugal fan for higher internal flow rate," *Journal of Mechanical Science and Technology*, vol. 27, no. 8, pp. 2263–2273, Aug. 2013, https://doi.org/10.1007/s12206-013-0609-6.

[14] P. N. Son, J. W. Kim, S. M. Byun, and E. Y. Ahn, "Effects of inlet radius and bell mouth radius on flow rate and sound quality of centrifugal blower," *Journal of Mechanical Science and Technology*, vol. 26, no. 5, pp. 1531–1538, May 2012, https://doi.org/10.1007/s12206-012-0311-0.

[15] A. P. Singh, Akshayveer, A. Kumar, and O. P. Singh, "Designs for high flow natural convection solar air heaters," *Solar Energy*, vol. 193, pp. 724–737, Nov. 2019, https://doi.org/10.1016/j.solener.2019.10.010.

[16] A. P. Singh, A. Kumar, Akshayveer, and O. P. Singh, "Effect of integrating high flow naturally driven dual solar air heaters with Trombe wall," *Energy Conversion and Management*, vol. 249, Dec. 2021, Art. no. 114861, https://doi.org/10.1016/j.enconman.2021.114861.

[17] A. P. Singh, A. Kumar, Akshayveer, and O. P. Singh, "Natural convection solar air heater: Bell-mouth integrated converging channel for high flow applications," *Building and Environment*, vol. 187, Jan. 2021, Art. no. 107367, https://doi.org/10.1016/j.buildenv.2020.107367.

[18] A. P. Singh, A. Kumar, Akshayveer, and O. P. Singh, "A novel concept of integrating bell-mouth inlet in converging-diverging solar chimney power plant," *Renewable Energy*, vol. 169, pp. 318–334, May 2021, https://doi.org/10.1016/j.renene.2020.12.120.

[19] H. G. Araya and S. T. Teferi, "Performance comparison of cylindrical and diverging solar chimney power plants," *Results in Engineering*, vol. 26, June 2025, Art. no. 105485, https://doi.org/10.1016/j.rineng.2025.105485.

[20] C. Ye *et al.*, "Enhanced Ventilation and Energy Efficiency of an Optimized Double-Channel Solar Chimney," *Buildings*, vol. 15, no. 8, Jan. 2025, Art. no. 1380, https://doi.org/10.3390/buildings15081380.

[21] G. Gan, "Impact of computational domain on the prediction of buoyancy-driven ventilation cooling," *Building and Environment*, vol. 45, no. 5, pp. 1173–1183, May 2010, https://doi.org/10.1016/j.buildenv.2009.10.023.

[22] W. Mbarek, R. Nciri, F. Nasri, C. Ali, and H. Ben Bacha, "Design and analysis of a novel solar hybrid air conditioning-ventilation-HDH desalination system," *International Journal of Ventilation*, vol. 20, no. 1, pp. 34–49, Jan. 2021, https://doi.org/10.1080/14733315.2019.1698166.

[23] S. Alimi, R. Nciri, F. Nasri, Y. A. Rothan, and C. Ali, "Performance investigation of an original hybrid solar façade system used for HDH desalination and building natural ventilation," *Journal of Building Engineering*, vol. 42, Oct. 2021, Art. no. 102515, https://doi.org/10.1016/j.jobe.2021.102515.

[24] R. Khanal and C. Lei, "A numerical investigation of buoyancy induced turbulent air flow in an inclined passive wall solar chimney for natural ventilation," *Energy and Buildings*, vol. 93, pp. 217–226, Apr. 2015, https://doi.org/10.1016/j.enbuild.2015.02.019.

[25] J. Kong, J. Niu, and C. Lei, "A CFD based approach for determining the optimum inclination angle of a roof-top solar chimney for building ventilation," *Solar Energy*, vol. 198, pp. 555–569, Mar. 2020, https://doi.org/10.1016/j.solener.2020.01.017.

[26] *ANSYS FLUENT 12.0. Theory Guide 67*. Canonsburg, PA, USA, 2009.